

Visualization of Vapor Film Collapse Behavior with Complexity on Quenching Process by Cellular Automaton

Tsuyoshi Sugimoto

Mechanical Systems Engineering Department, National Institute of Technology, Asahikawa College, Asahikawa 071-8142, Japan

Abstract: The vapor film collapse that occurs in the quenching process is complicated and affects the heat treatment quality and its distortion. In order to incorporate it into the MBD (Model Based Development) technology required these days, it is necessary to predict the quality of heat treatment by CAE (Computer Added Engineering), shorten the product development period. The calculation of the vapor film collapses in a simple and practical time in order to improve the product performance. However, in the past, in order to formulate the vapor film collapse on a simulation, it was necessary to perform a very large amount of computational calculation CFD (computational fluid dynamics), which was a problem in terms of computer resources and the model of vapor film collapse. In addition, this phenomenon has a complexity behavior of the phenomenon in iterative processing, which also complicates the calculation. In this study, the vapor film collapse phenomenon is easily visualized using self-organized cellular automaton simulation which includes the phenomena of “vapor film thickness and its fluctuation”, “flow disturbance”, “surface step of workpiece”, and “decrease of cooling due to r shape of surface”. The average cooling state and repeated fluctuations of the cooling state were reproduced by this method.

Key words: Quenching, cellular automaton, vapor film collapse, complexity.

1. Introduction

For the purpose of improving the strength and life of metal parts such as gears, carburized quenching using a liquid quenching agent such as oil/water is performed to improve the bending or wear strength. While carburized quenching shows a significant improvement in strength compared to non-treatment agents, shape accuracy deteriorates due to heat treatment deformation, etc., causing noise during operation. Such deformation is called as heat treatment deformation. Post-processing such as finish grinding is performed to correct heat treatment deformation, but post-processing costs hundreds of billions of yen in Japan [1]. In order to reduce this cost, it is beneficial to predict the tendency and amount of heat treatment deformation in advance

and feed it back to the pre-machining shape, and to set the optimum heat treatment deformation through the process [2].

Because of longer heat treatment time than that of other processes, it is often carried out in a group processing and variations in heat treatment deformation occur within the processing lot and between processing lots, which is a process that appropriately considers the heat treatment deformation. It makes process design difficult. In response to the growing expectations for model-based development technology in recent years [3, 4], heat treatment simulation technology is also included in this study, in order to carry out a simulation that reproduces heat treatment deformation and its variation within an economically beneficial time, we develop a cellular automaton simulation including

Corresponding author: Tsuyoshi Sugimoto, Ph.D. of Engineering, Associate Professor, research fields: heat treatment, material process, computational simulation.

vapor film collapse phenomena that simulate a low-dimensional space and verify its effectiveness [5].

2. Low Dimension Cellular Automaton for Vapor Collapse Phenomena

2.1 Observation for Collapse of Vapor Film

As the formulation of the cellular automaton, oil quenching was performed on the test piece in order to clarify the cooling phenomenon that occurs during quenching, and changes in the vapor film movement that occur on the surface of the test piece were observed.

The test piece used was a round bar of $\phi 20$ mm \times length 60 mm, made by JIS SCr420H, and the quenching was JIS Class 2 No. 1 oil Idemitsu Kosan High Temp X, an oil temperature of 100 °C with still state. The quenching phenomenon consists of three stages: a vapor blanket stage in which the surface of the test piece is completely covered with a vapor film, a boiling stage in which the vapor film breaks and bubbles adhere to the surface of the test piece, and a convection stage in which the surface of the test piece is covered with only liquid. Figs. 1a, 1b, and 1c show the figures in which the transition to each stage is different depending on the part of the test piece, but the whole is dominant in each stage. Looking at the boiling stage in Fig. 1a, the test piece is entirely covered with a vapor film, and the surface of the vapor film is vibrating. Therefore, the thickness of the vapor film fluctuates with the elapse of time. Looking at Fig. 1b, the vapor film starts to break from the edged part at the lower end of the test piece. Looking at Fig. 1c, bubbles are

formed under the test piece. It is thought that this is because the generated vapor and the air that existed before quenching cannot escape from the lower end and remain.

In order to verify what the cooling state will be in the case of quenching including the phenomenon of vapor film collapse, JIS No. 2 type 1 Idemitsu Kosan High Temp X quenching oil, an oil temperature of 100 °C with still state for a tetragonal shape made of 30 mm \times 40 mm \times 40 mm JIS SUS304 stainless steel [6]. Based on the heat transfer coefficient shown by “Estimated silver prove” in Fig. 2, the heat transfer coefficient indicating the cooling state of each surface and corner was derived by the inverse problem method. The results are shown in same figure. The heat transfer coefficient at the bottom and corners differs greatly from the value of “Estimated silver prove”, and at the bottom, the peak at the boiling stage is small and heat insulation is strong. At the corners, it can be seen that the boiling stage changed to a high temperature and the vapor film collapsed at an early stage. This corresponds to the observation results obtained in Fig. 1, and it can be said that it is important to reproduce the phenomena at the bottom and corners to reproduce the quenching cooling phenomenon on the simulation.

2.2 Examination of Quenching Cooling

We examine a method for formulating quench cooling based on the behavior of vapor films. The heat transfer coefficient curve with high heat transfer in the middle region and high boiling stage as seen in Fig. 2 is due to the adiabatic insulation of the vapor film [7].

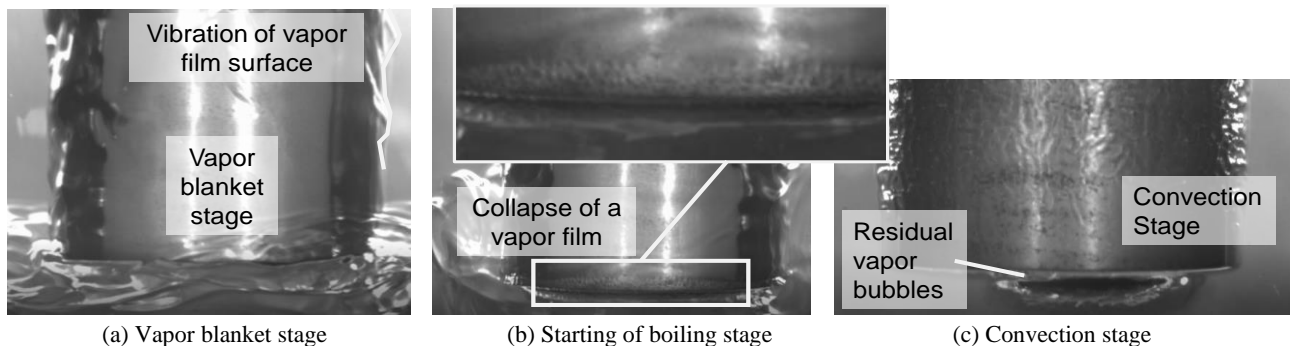


Fig. 1 Observation results of quenching on cylinder shape piece.

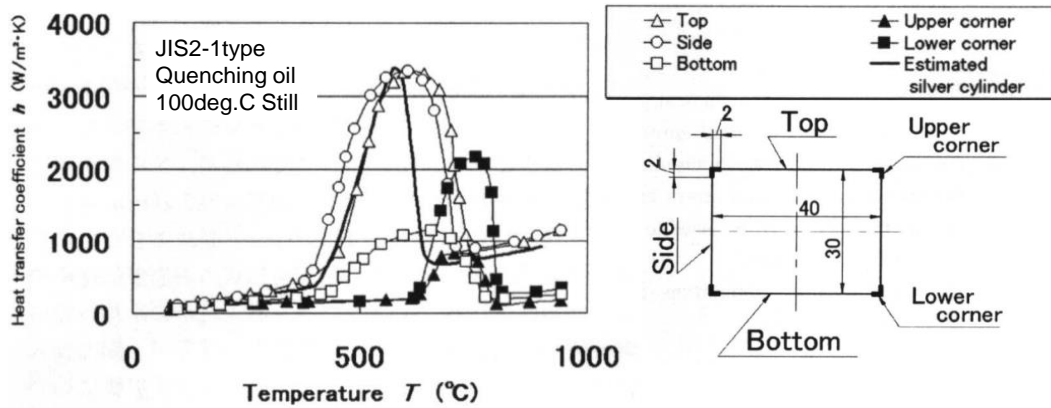


Fig. 2 Change of heat transfer coefficient in quenching on box shape.

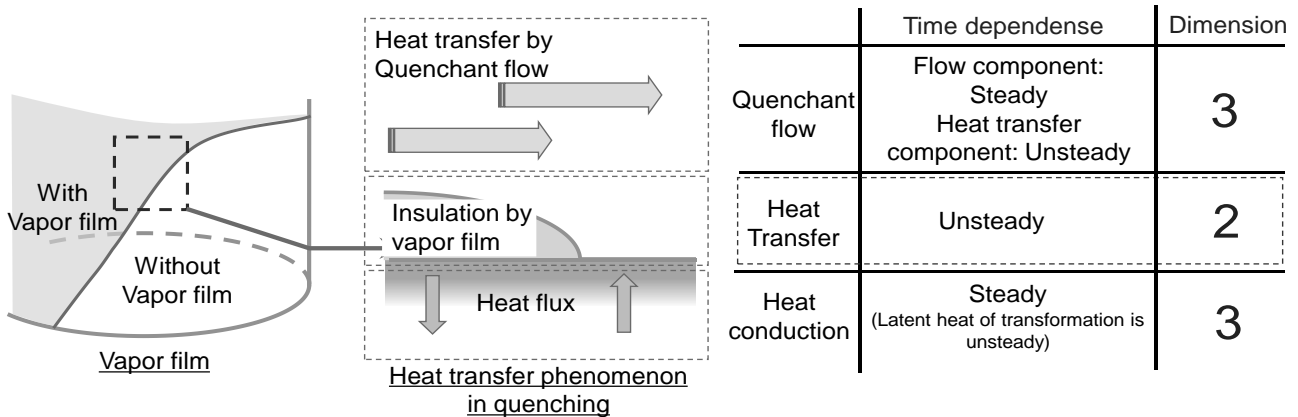


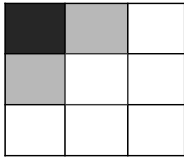
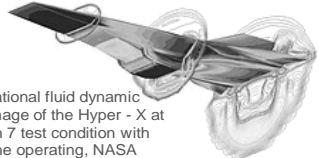

Fig. 3 Schematic of quenching phenomena.

Fig. 3 summarizes the characteristics of various phenomena seen in quench cooling. The quenching cooling phenomenon is classified into heat conduction inside the object, heat transfer on the surface of the object, and heat transport outside the object from the inside of the object on quenching. Each phenomenon is classified into a stationary phenomenon or a non-stationary phenomenon, and the phenomenon is classified into two-dimensional or three-dimensional, and is shown in the table in Fig. 3. Here, in quenching, heat conduction inside the object and quenching agent transport and heat transport outside the object are three-dimensional phenomena and are generally stationary phenomena. On the other hand, heat transfer that occurs on the surface of an object is a non-stationary phenomenon. From this, many constitutive equations for complex phenomena [8] are required for analysis of vapor film collapse phenomenon during quenching by FEM (Finite Element Method) or FDM (Finite Difference Method).

It is considered that a very expensive calculation cost will be incurred if the heat transfer phenomenon on the surface of the object is solved by the same method as the phenomenon inside and outside the object.

Complex phenomena including low-dimensional, phase transformations such as heat transfer in the quenching process occur discontinuously. When the phenomenon is reproduced analytically, the convergence is poor and the speed is generally low, so the calculated area is often very small. Table 1 shows a comparison between the cellular automaton methods using this research and the FEM/FDM that is generally used to reproduce heat transfer and fluid phenomena. The cellular automaton method has the feature that it is possible to solve phenomena containing multi-phases with a small number of calculation lattices under complicated boundary conditions with high convergence, and it can be said that it is suitable for solving quenching phenomena.

Table 1 Comparison of advantages of cellular automaton method and FEM/FDM.

	Cellular Automaton	FEM/FDM
		 <p style="font-size: small;">Computational fluid dynamic (CFD) image of the Hyper - X at the Mach 7 test condition with the engine operating, NASA</p>
 Advantages		
Number of calculation lattice	Low	High
Time step	Small	Large
Convergence(Calculation cost)	Complete	Incomplete
Complex boundary conditions	Easy	Possible
Multi phase	Easy	Possible
Moving	Difficult	Easy
High dimension	Difficult	Easy

3. Formulation of Cellular Automaton on Vapor Collapse Phenomena in Quenching Process

The vapor film collapse phenomenon and the change in heat transfer coefficient during quenching were described in the cellular automaton according to the contents of the above-mentioned investigation of the mode. Cellular automaton describes the phase of the film covering the surface and the temperature of the surface of the component. With reference to the research results on coagulation by Oono et al. [9], described a similar phenomenon by Wolfram [10] and Paul et al. [11], the phase change is in the vicinity of Neumann, which is affected by the cells of interest, up, down, left, and right, and the temperature is up, down, left, and right, as well as the upper right, upper left, and lower right, the vicinity of Moore, which is also affected by the lower left, was adopted. As a result, it is possible to reproduce the state of the gently covered vapor film in which the state of the vapor film changes in a staggered arrangement for the phase.

For the phase, the vapor film stage, boiling stage and convection stage are set to 0, 1, 2 respectively, and the actual temperature of the surface is described for the temperature. Fig. 5 shows the heat transfer coefficient curve when there are no factors that change the state of the vapor film such as disturbance. It is available from

each oil manufacturer and public database. In Japan, it is published on the website of the *Japan Society of Heat Treatment Association* [12]. T_b , which transitions from the vapor blanket stage to the boiling stage, and T_c , which transitions from the boiling stage, are defined from the heat transfer coefficient curve, and the transitions are shown in Eqs. (1) and (2). The transition from the vapor film stage to the boiling stage shows the ease of transition. b is shown in (i), (ii) and (iii).

For temperature changes, in addition to heat transfer in the direction parallel to the surface, a Newton cooling term that controls the heat transfer coefficient and quenchant temperature from the surface was added.

Phase Change:

Transition to the boiling stage:

$$S_0^t = 0 \text{ and } \sum_{i=1-4} S_i^t \geq b \text{ and } T_0^t \leq T_b \text{ then} \\ S_0^{t+1} = 1, T_0^{t+1} = T_0^t - \alpha \quad (1)$$

Transition to the convection stage:

$$S_0^t = 1 \text{ and } T_0^t \leq T_c \text{ then} \\ S_0^{t+1} = 2, T_0^{t+1} = T_0^t - \beta \quad (2)$$

Temperature Change:

$$T_0^{t+1} = T_0^t + \left\{ \frac{1}{6} (T_1^t + T_2^t + T_3^t + T_4^t) \right. \\ \left. + \frac{1}{12} (T_5^t + T_6^t + T_7^t + T_8^t) \right. \\ \left. - k \cdot T_e \right\} \quad (3)$$

α, β : Latent heat

b : factors for vapor blanket collapse

T_e : quenchant temperature

T_b, T_c, k : shown in Fig. 5

k is heat transfer coefficient

(i) Vibration of vapor film surface

Eq. (4) was created by incorporating the fluctuation of the vapor film thickness due to the vibration caused by the surface tension [13] and the disturbance of the flow. γ is a factor that vibrates the vapor film, which is determined by the aspect of the flow. A normal distribution is shown as shown in Fig. 6. N has a probability distribution with Markov property with previous time step and also has continuity with Moore neighborhood cells.

$$b = b_0 + \gamma N(\mu, \sigma^2) \quad (4)$$

γ, μ, σ : Control parameter for vapor film vibration

(ii) Reduction of vapor film thickness due to edge shape

At the edge, the vapor film thickness becomes thinner due to the influence of surface tension at the gas-liquid interface of the vapor film, and the vapor film collapse is promoted [14]. This is described by Eq. (5).

$$b = b_0 + \delta \quad (5)$$

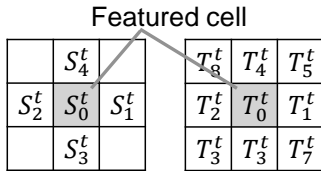
δ : Vapor film collapse due to edge

(iii) Effect of surface tilt

Eq. (6) describes that the air remaining in the steam film and the hardened oil stays on the lower surface and the cooling is hindered.

$$b = b_0 - \varepsilon \cos(\theta) |_{\theta \leq 0} \quad (6)$$

ε : Tilt of surface (Horizontal: 0, downward is minus)



(i) Phase (ii) Temperature

S_i^t : Phase 0: Vapor blanket stage t :Time
 1: Boiling stage i :Position
 2: Convection stage

T_i^t : Temperature

Fig. 4 Cell automaton of phase and temperature.

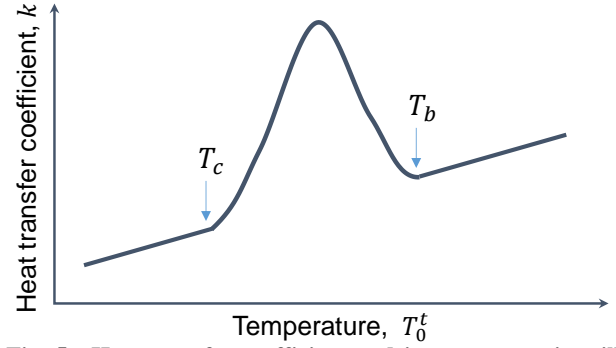


Fig. 5 Heat transfer coefficient and its parameter in still quenching condition.

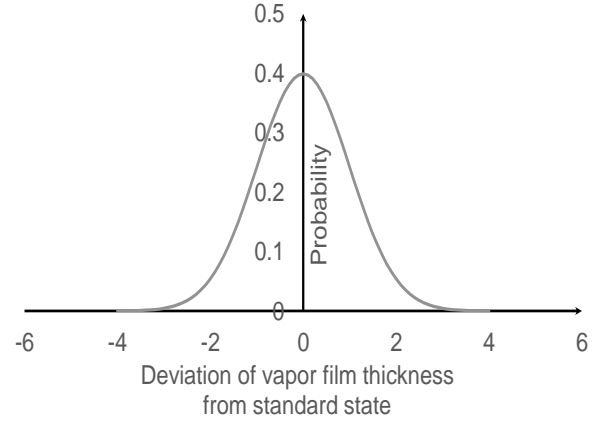


Fig. 6 Deviation of vapor film thickness from standard state.

4. Experimental Procedure

We verified whether the cooling state could be reproduced using a cellular automaton whose constitutive equation was examined. Using Microsoft Excel 2019 and Visual Basic for Applications, the state transition from $t-1$ step to t step over a unit time is described in Eqs. (1)-(6). When the calculation in all one step is completed, the result in t step is transferred to the worksheet in $t-1$ step, and the calculation of the next unit time is executed again. The calculation of the number of steps up to the predetermined finish time was completed, and when the end time was reached, the calculation was completed. At this time, the “Wait” command was described during the calculation so that the real time and the calculation time would be almost the same.

Since the calculated cooling curve shows the heat flux per unit area, it can be treated as the heat transfer

Visualization of Vapor Film Collapse Behavior with Complexity on Quenching Process by Cellular Automaton

coefficient as it is by correcting the curvature of the surface and differentiating it with time. Therefore, the heat transfer coefficient of each part was calculated from the calculated cooling curve.

In order to compare with the calculation results, the cooling state was calculated with various coolants and test pieces, and the heat treatment deformation was calculated especially under the asymmetrical boundary conditions where the surroundings were disturbed.

5. Result

Regarding the created cellular automaton, the vapor film collapse was reproduced with a simple cylindrical test piece. The test piece used was a $\phi 20 \text{ mm} \times 60 \text{ mm}$ cylinder bar and the material was JIS SCr420H. A transparent version of Idemitsu Kosan JIS No. 2 type 1

quenching oil, was used, and the cylinder was heated to $850 \text{ }^\circ\text{C}$ before quenching. The results are shown in Fig. 7a and 7b show the state of vapor film collapse and the results of temperature distribution by simulation obtained by cellular automaton. The timing of the measurement was the stage when the vapor film collapse started. In both the experiment and the simulation, it was reproduced that the lower half preferentially moved to the boiling stage.

Next, a quantitative evaluation of the cooling state was performed by this simulation. The simulation results by this method and the actual cooling state were compared with the silver bar cooling test results by the JIS K2242A method shown in Fig. 8a and 8b which show the results for JIS No. 1 type 1 oil and No. 2 type 2 oil. Both experimental and simulation results showed good agreement.

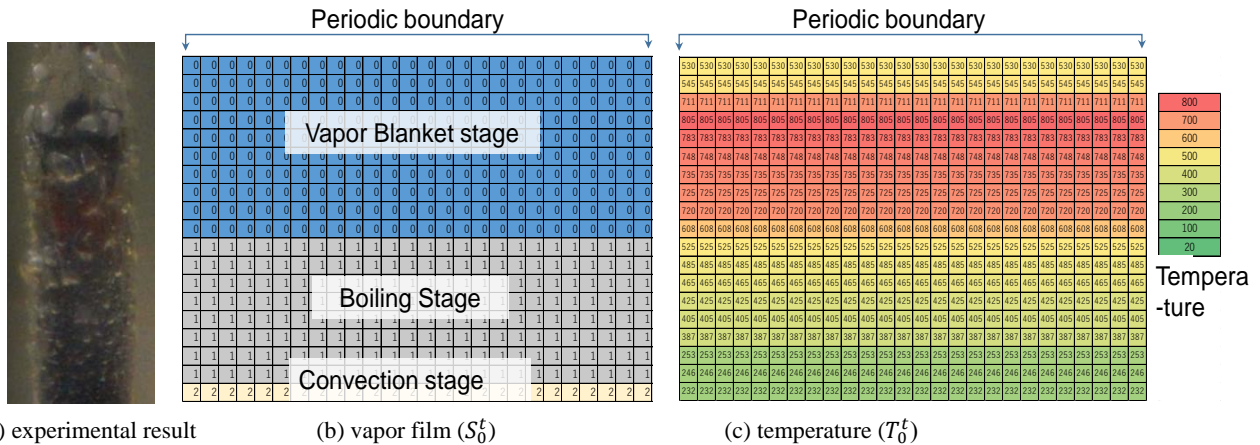


Fig. 7 Quenching results with cylindrical pieces in still condition at starting of convection stage.

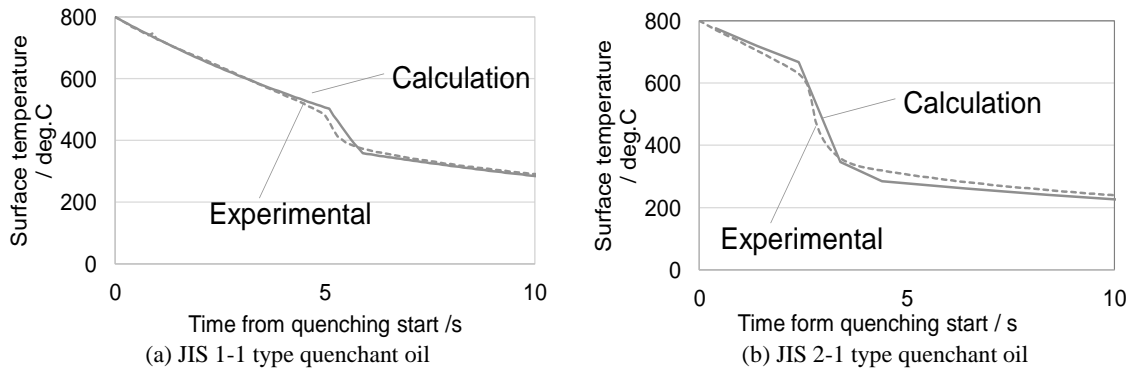


Fig. 8 Comparison of calculated cooling curve with experimental.



Fig. 9 Comparison of cooling curve with experiment.

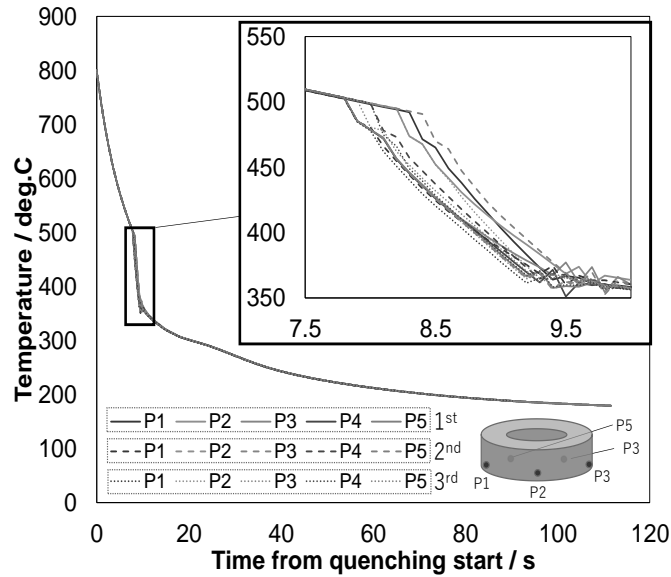


Fig. 10 Comparison of cooling curve in three times calculation.

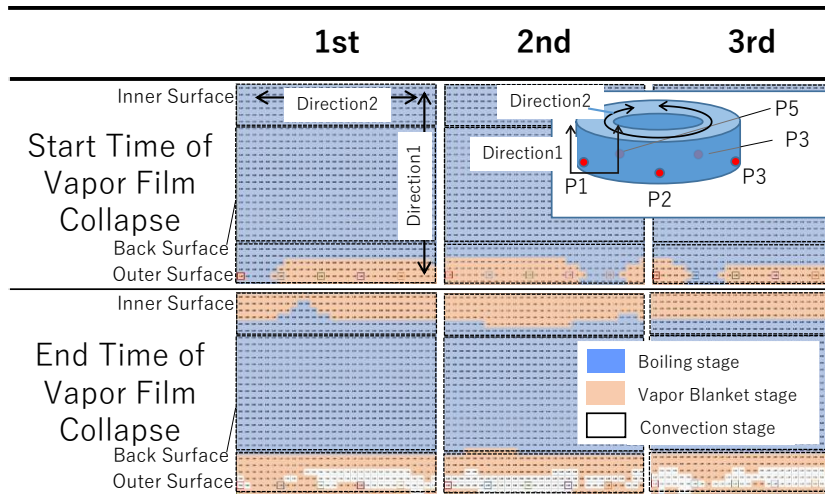


Fig. 11 Vapor film collapse mode in three times quenching.

Fig. 9 shows the collapse of the steam film when a ring-shaped gear is quenched. A vapor film collapse has started from a part of the side surface, and the collapse is spreading to both sides. At the inner diameter and the back surface, vapor film collapse

progressed at a later stage. The starting point of collapse was not constant in repeated quenching.

The calculated vapor film collapse mode for ring-shaped piece was shown in Fig. 10. Three times calculations were performed, and the cooling conditions at the lower

part of the outer periphery of each ring are indicated by P1-P5 in Fig. 11. The cooling curves were almost the same for quenching at 15 curves (5 points \times 3 times). However, there were 15 differences in the start timing of vapor film collapse, the cooling curve at the boiling stage, and the subsequent cooling curve.

In particular, the range of variation in the cooling time of P1-P5 was almost the same in the three quenching cycles, but the cooling order varied among the three quenching cycles.

Fig. 11 shows the state of the vapor film collapse on the surface around the ring shape obtained by three cooling calculations at the beginning of the collapse of the steam film. The location of the collapse of the vapor film at the beginning of the collapse varied with three quenching cycles, but the collapse shape around the beginning of the collapse became similar. The vapor film collapse occurred first on the outer surface, and then on the inner surface. This is thought to be due to the fact that the outer circumference is convex outward, so cooling occurs first.

6. Discussion

By using a cellular automaton using simple parameters, it was possible to obtain the heat transfer coefficient and vapor film collapse mode distribution during quenching in a calculation time close to the actual phenomenon. This may allow us to describe various phenomena related to heat treatment variations in a wider variety of ways.

In the future, we would like to improve this cellular automaton so that it can directly correspond to the actual heat treatment conditions, and also make it possible to calculate fluctuations in the quality of repeated heat treatments and the quality distribution in the packaging.

7. Conclusion

Conventionally, the vapor film collapse that occurs during quenching has asymmetry due to repeated fluctuations, and it has been suggested that this is a

member of complicated heat treatment deformation. In this study, we succeeded in reproducing this asymmetry and fluctuation repeatedly in practical time using a cellular automaton. This suggests that the heat treatment deformation may be caused by the instability of the vapor film collapse.

References

- [1] Kinki Bureau of Economy, Trade and Industry. 2009. "By Simulation Utilization Technology Development of Advanced Heat Treatment Method." Accessed May 10, 2022. <https://www.chusho.meti.go.jp/keiei/sapoin/portal/seika/2006/18-40-16-5.pdf>. (in Japanese)
- [2] Brinksmeier, E., Lübben, T., Fritsching, U., Cui, C., Rentsch, R., and Sölter, J. 2011. "Distortion Minimization of Disks for Gear Manufacture." *International Journal of Machine Tools and Manufacture* 51 (4): 331-8.
- [3] Fujikawa, S. 2013. "Model Based Development in Mazda." *Mazda Technical Review* 31: 44-7.
- [4] He, X. G., Hua, E. T., Lin, Y., and Liu, X. Z. 2011. "Based Automotive Products Process Planning Technology." *Applied Mechanics and Materials* 88-89: 570-5.
- [5] Sugimoto, T., Taniguchi, K., Yamada, S., and Matsuno, T. 2018. "Calculation Method between Heat Treatment Simulation and Computer Fluid Dynamics." *Materials Performance and Characterization* 8 (2): 37-49.
- [6] Narazaki, M. 2006. "Actually and Scope on Simulation of Heat Treatment II: Cooling Characteristic and Database." *Journal of the Society of Material Science* 55 (6): 589-94.
- [7] Narazaki, M., Kogawara, M., Shirayori, A., and Fuchizawa, S. 2003. "Effect of Heat Transfer Coefficients on Simulation Accuracy of Quenching of Steel." *Journal of the Visualization Society of Japan* 23 (2): 197-200.
- [8] Arai, T., and Furuya, M. 2007. "Effect of Salt Additives to Water on the Severity of Vapor Explosions and on the Collapse of Vapor Film." *Thermal Science & Engineering* 15 (3): 91-100.
- [9] Oono, Y., and Puri, S. 1987. "Computationally Efficient Modeling of Ordering of Quenched Phases." *Phys. Rev. Lett.* 58 (8): 836-9.
- [10] Wolfram, S. 2007. *A New Kind of Science*. Champaign, IL: Wolfram Store.
- [11] Paul, G., Seybold, A. B. E., Matthew, J., O'Malley, A., Lemont, B., Kier, C., and Cheng, C. K. 2006. "Cellular Automata Simulations of Vapor-Liquid Equilibria." *Australian Journal of Chemistry* 59 (12): 865-8.
- [12] Japan Society of Heat Treatment. 2016. "Quenchant Database for Heat Treatment Simulation." Accessed May, 2022. <https://jsht.or.jp/study/>.

- [13] Kanatani, K. 2009. "Interfacial Instability Induced by Lateral Vapor Pressure Fluctuation in Bounded Thin Liquid-Vapor Layers." *Physics of Fluids* 22: 1-38.
- [14] Abe, Y., Matsukuma, Y., and Tochio, D. N. 2008. "Numerical Simulation of Vapor Film Collapse Behavior on High-Temperature Droplet Surface with Three-Dimensional Lattice Gas Cellular Automata." *Transactions of the Atomic Energy Society of Japan* 7 (4): 321-7.